Proceedings World Geothermal Congress 2020+1
Reykjavik, Iceland, April - October 2021

Seismic Feasibility Study to Identify and Characterize Supercritical Geothermal Reservoirs Using DTS, DAS, and Surface Seismic Array

Junzo Kasahara[1,5], Yoko Hasada[1,2], Haruyasu Kuzume[1], Yoshihiro Fujise[3], Hitoshi Mikada[4], and Keigo Yamamoto[6]

1: ENAA, Toranomon Marine Building 10th, 3-18-19, Toranomon, Minato-ku, Tokyo 105-0001, Japan

2: Daiwa Exploration and Consulting Co. Ltd., 5-10-4 Toyo, Koto-ku, Tokyo 135-0016, Japan

3: WELMA Co. Ltd., 2-3-3, Watanabe street, Chuo-ku, Fukuoka 810-0004, Japan

4: Kyoto University, Department of Earth Resources Engineering, Katsura, Nishikyo-ku, Kyoto 615-8530, Japan

5: Shizuoka University, Center for Integrated Research and Education of Natural Hazard, 836 Ohya, Shizuoka, Japan

6: Kyoto University, Sakurajima Volcano Research Center, Sakurajima, Kagoshima 891-1419, Japan

kasahara.junzo@shizuoka.ac.jp

Keywords: Supercritical water, DAS, geothermal field, reservoir imaging, seismic method, time lapse, monitoring

ABSTRACT

To image supercritical water reservoirs, we propose the use of the following methods: distributed acoustic sensor (DAS) for the borehole, surface seismic array, active or passive seismic sources, and full-waveform inversion. To evaluate our approach, we carried out a feasibility study in the Medipolis geothermal field located in Kyushu Island, Japan. We deployed an optical fiber down to a depth of 977 m in the borehole. Using distributed temperature sensing mode, the measured temperature at a depth of 914 m was 264 °C. We obtained 4.5 days of continuous seismic data using DAS and surface seismometers. The DAS data were obtained every 1 m from the depth of 977 m to the ground surface. We observed seven natural earthquakes. The sensitivity was comparable with the surface seismometer measurements, which suggested that the optical-fiber deployment in the exiting borehole could provide reasonable coupling to the borehole casing. We obtained the apparent interval Vp profile along the borehole. Estimated interval Vp exhibited large discrepancies for cases between the north and south incidents. Earthquakes in the south demonstrated lower Vp of approximately 3.0 km/s from a depth of 1,000 m to the wellhead. On the other hand, earthquakes in the north exhibited Vp of 4.5 km/s at a depth of 1,000 m and 3.0 km/s in the shallow part. The discrepancies could be explained when the deviation in the borehole and the incident angles and azimuths were considered. No distinct seismic attenuation was observed even in the high-temperature zone, and Vp in the high-temperature zone was estimated to be 3.0 km/s. A P-to-S converted phase was evident on the surface seismometers, which could indicate the presence of a conversion zone around the 4-km depth beneath the Medipolis geothermal field. We also identified kicks that traveled at 5 km/s, probably through the casing pipes. The cause of the kicks is being analyzed.

1. INTRODUCTION

Geothermal energy has become one of the most important energy sources. Supercritical water has attracted the attention of the geothermal community as an important future renewable-energy source in the world (Dobson *et al*., 2017; Reinsch *et al.*, 2017). In Japan, the New Energy and Industrial Technology Development Organization (NEDO) is promoting supercritical geothermal exploration as an important future energy source. Kasahara *et al*. (2018a) examined the possibility of using supercritical water as geothermal energy for electric power. In the Kakkonda geothermal field in Japan, the scientific drilling of WD-1a geothermal well in 1995 revealed that the temperature was above 500 °C at the depth of 3,800 m (Muraoka *et al.*, 1998). Because the critical points of pure water are 373.95 °C and 22.064 MPa, the Kakkonda well was believed to reach the supercritical condition at the depth of 3,800 m, although it appeared to be unfortunately dry (Muraoka *et al.*, 1998). On Earth, many geothermal fields exist that show conditions close to the supercritical point of water or above (Dobson *et al*., 2017; Reinsch *et al.*, 2017). The drilling well in Larderello, Italy demonstrated 507–517 °C at the depth of 2.9 km, but it is in a dry state (Bertani *et al.*, 2018). A question remains whether the drilling in Larderello reaches the K-horizon or not (Rabbel, 2019). Therefore, learning the physical properties of potential supercritical zone before and/or during the drilling using other methods than drilling is important.

Knowing the physical properties of a geothermal reservoir without drilling is difficult. Recently, in enhanced geothermal systems several efforts have been exerted to use a fiber-optic distributed temperature sensor (DTS) and distributed acoustic sensor (DAS) technologies (Hartog, 2017; Patterson, *et al*., 2018; Mellors *et al*., 2018; Trainor-Gutton, *et al*., 2018). The DTS method senses the temperature using the Raman or Brillouin scattering modes of light in the optical fiber. The DAS method senses the strain (strain rate) using the Rayleigh scattering mode, which represents the backscattering of an input laser light due to seismic-wave arrivals (Hartog, 2017). The sensing interval is quite short, which is within a few meters. Because the temperature at the supercritical point is 373.95 °C, ordinal seismometers cannot be used in the deeper part of the borehole. DAS, which uses an optical fiber, can be used in high-temperature conditions of as high as 500 °C, although coating the fiber using an appropriate skin is necessary to avoid hydrogen invasion.

For imaging of oil and gas reservoirs, we use the backpropagation method such as the time-reversal method (Kasahara and Hasada, 2016) where a receiver array acts as pseudo-seismic sources and DAS to provide dense seismic sources in the imaging of supercritical water reservoirs. In our approach, we design the method using active and/or passive seismic sources as well as the DAS and full-waveform inversion (FWI) method (Kasahara *et al*., 2018b, c, 2019a) (Figure 1). We can image the temporal change in the supercritical water caused by the migration in geothermal reservoir and perform hydrofracturing to create new geothermal reservoirs

and generate geothermal heat. Therefore, we propose the seismic time-lapse technology to learn the physical properties of a supercritical water reservoir.

In 2017–2018, we evaluated the quality of DAS data in the field and recognized that DAS could provide comparable seismic signals similar to ordinal seismometers, although the current DAS sensitivity is slightly less compared with the seismometer sensitivity (Kasahara *et al.*, 2018c, d). Even though we are aware of this disadvantage, DAS can still provide very dense data, namely, an interval of a few meters.

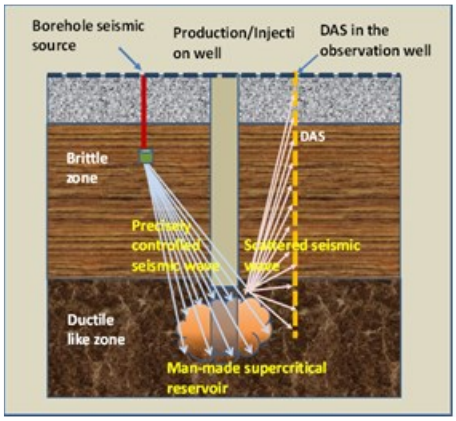

Figure 1: Seismic monitoring method to image natural and/or man-made supercritical reservoir(s) using borehole seismic source, DAS array in the borehole, and surface seismic array.

To determine the physical properties using the observed data, we carried out simulations using the FWI method assuming active seismic sources and natural earthquakes (Kasahara *et al*., 2018b, 2019a). The physical properties such as Vp, Vs, and density in the reservoir were clearly revealed when the active seismic source was at a depth of 2 km and the distance from the DAS array was 3 km. We also studied natural earthquakes as seismic sources to image deep-seated igneous intrusions at the deep of 4 km. We clearly illustrated the image of the intrusion (Kasahara *et al*., 2019a), but the assumed values of Vp, Vs, and density were not fully retrieved (Kasahara *et al*., 2018c).

To evaluate the usefulness of our approach in a real geothermal field, we carried out a feasibility study in the Medipolis geothermal field located in Kyushu Island, Japan, in November 2018 (Figure 2). In this study, we did not use an active seismic source but used natural earthquakes that occurred near the geothermal field.

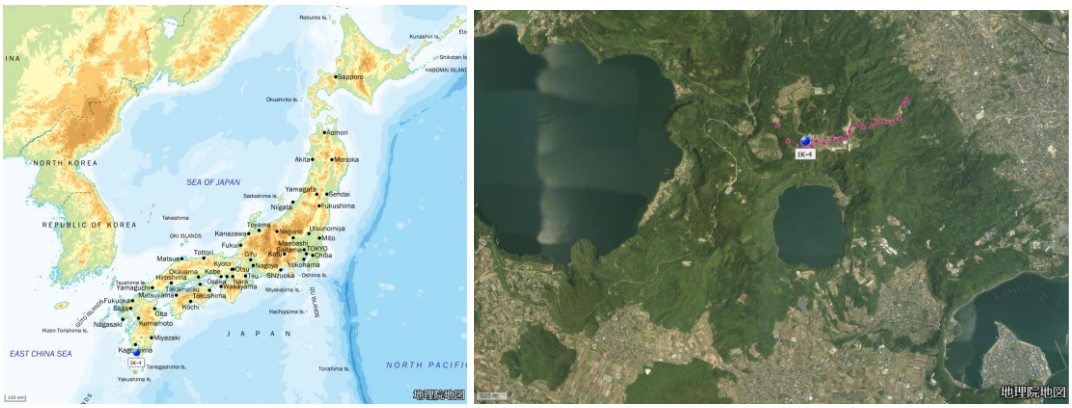

Figure 2: (Left) Japanese islands and (blue circle at the bottom) Medipolis geothermal field. (Right) Medipolis geothermal field at the upper right. The IK-4 well is indicated by a blue dot, and the surface seismometers are indicated by red triangles. The seismometer spacing is 100 m. The maps are from GSJ.

2. FEASIBILITY STUDY AT THE MEDIPOLIS GEOTHERMAL FIELD

The Medipolis geothermal field was studied by NEDO (NEDO, 2008, 2009, 2010). The 3D view of the five wells in this geothermal field studied by NEDO (2008, 2009, 2010) is shown in Figure 3. The temperatures at depths of 700 and 1,000 m are higher than 200 °C. We used the IK-4 well. Currently, three active wells are present: IK-1 well for production, IK-3 well for reduction, and IK-4 well for observation. We used the IK-4 well for the DTS and DAS measurements. The Medipolis geothermal power plant generates 1.4 MW using the binary system. The depths of the three wells are 1,500 m. The wellheads of IK-1 and IK-4 are only a few tens of meters apart. The bottoms of the two wells are only 200 m apart. Steam is continuously produced during the DAS study. The steam production is taken from a depth of 1,200 m in the IK-1 well. The IK-4 well is vertical down to 500-m deep and deviates toward the west from the depth of 500 to 1,500 m.

The feasibility study was carried out in November 2018. An optical fiber was deployed down to the depth of 977 m in the IK-4 borehole. The upper 240 m of the borehole was filled with air, and the rest was filled with water. The gauge length of the DAS

processing was 4 m, and seismic data at every 1 m were continuously obtained for 4.5 days at 1-kHz sampling. We also installed 20 sets of 3C short-period seismometers on the ground surface in the study field (Figure 2). The length of the surface seismic array was 2 km at a 100-m interval.

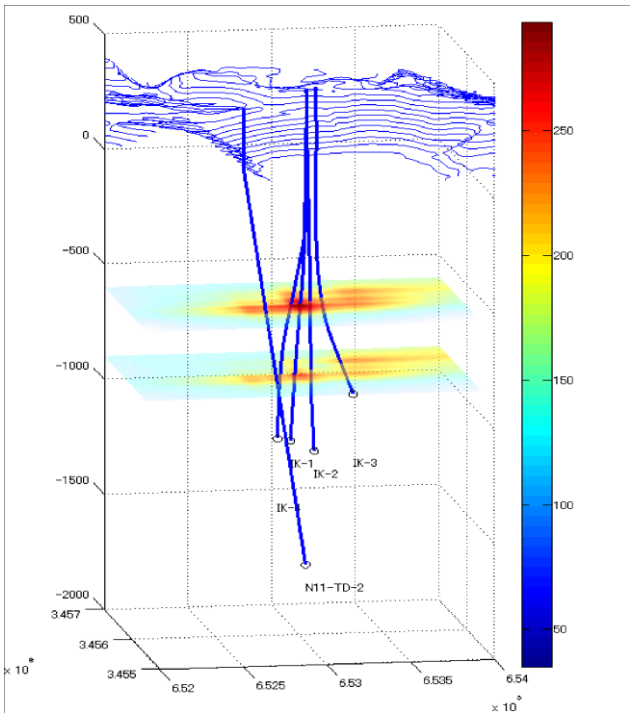

Figure 3: Temperature distribution based on five well data (NEDO, 2010). The temperatures at 700 and 1,000 m are higher than 200 °C.

3. RESULTS OF THE FEASIBILITY STUDY AT THE MEDIPOLIS GEOTHERMAL FIELD

3.1 Results of temperature measurement

Before the DAS data acquisition, we measured the temperature at DTS mode from a depth of 0 to 977 m in the borehole using the same fiber-optic cable as the DAS. Figure 4 shows that the maximum temperature was 264 °C at 914 m. This temperature was approximately the same as the measurement in 2008 (NEDO, 2010).

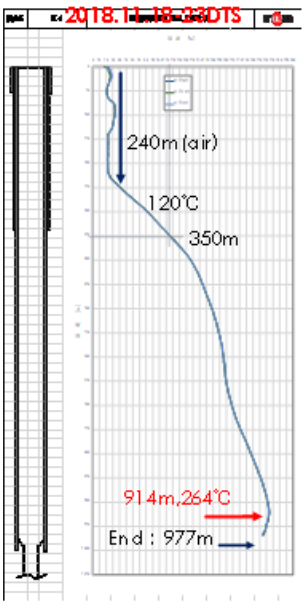

Figure 4: Temperature profile obtained by the DTS mode in the observed borehole. (Right) Measured temperature distribution in the borehole. The temperature at the depth of 914 m in the borehole was 264 °C. The DAS system used the same optical fiber with a 1-m-interval data acquisition. (Left) casing plan.

3.2 Results of the seismic measurements

We conducted the seismic measurement using the DAS mode and ground surface seismometers. Two of the surface seismometers near the production wellhead showed very large artificial noise of 30 and 57 Hz, but such noise was not observed by the DAS in the borehole.

For 4.5 days of continuous monitoring by DAS, we observed seven natural earthquakes from M = 0.8 to M = 5.2 (Table 1 and Figure 6). Two examples of the observed earthquake records (EQ5 and EQ1) are shown in Figures 6 and 7, respectively. The first arrivals of P of both earthquakes were observed at the entire depth from 977 to 0 m at every 1-m interval.

Table 1: List of earthquakes observed by DAS for 4.5 days. The area is shown in Figure 5.

	Origin time	Latitude	Longitude	Depth(km)	Magnitude	Area
EQ1	2018/11/20/03:16 28.7	31° 23.6'N	130° 37.1'E	10	1.4	C
EQ2	2018/11/20/19:34 52.2	29° 21.5'N	129° 48.4'E	65	4	D
EQ3	2018/11/20/22:02 42.3	31° 24.2'N	130° 34.3'E	14	0.9	C
EQ4	2018/11/20/23:09 01.5	31° 30.0'N	130° 42.4'E	119	2.3	E
EQ5	2018/11/21/04:09 49.9	30° 24.0'N	130° 9.0'E	123	5.2	A
EQ6	2018/11/21/04:59 29.1	30° 26.9'N	130° 9.1'E	123	3.1	B
EQ7	2018/11/21/17:49 18.0	31° 19.3'N	131° 42.7'E	22	2.7	F

Figure 5: Seven natural earthquakes in 2018 (Table 1) were observed by the DAS and surface seismometers in the geothermal field. A: near Tanegashima (EQ5), B: near Tanegashima (EQ6), C: Kagoshima Bay (EQ1, EQ3), D: near Tokara (EQ2), E: Ohsumi Peninsula (EQ4)), and F: east of Ohsumi Peninsula (EQ7)). The Medipolis geothermal field is located in the (blue circle) southern end of Kyushu Island. The map is from GSJ.

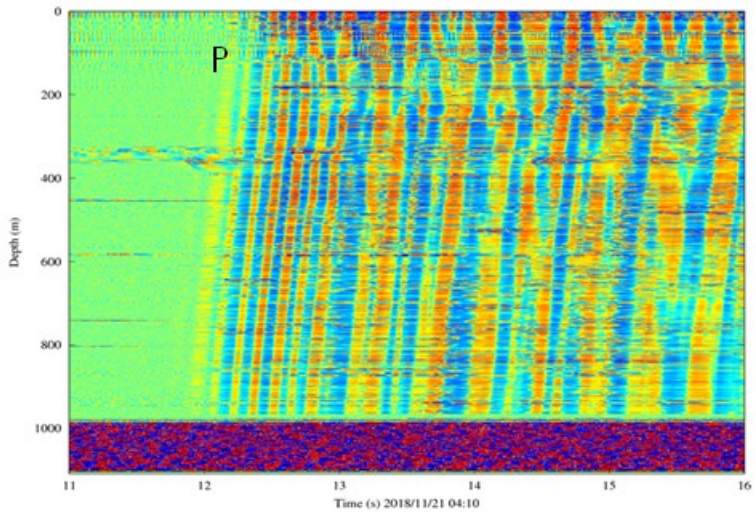

Figure 6: DAS records of EQ5 (M = 5.2) that occurred with recorded 100-km focal distance and 123-km focal depth. The vertical axis depth is from (top) 0 m to (bottom) 977 m. The horizontal axis indicates the arrival times in seconds. The P–S time of this earthquake is approximately 17 s. The part of the S arrivals is not shown in this figure.

We recognized the surface-reflected arrivals of the EQ5 earthquake (Figure 6). EQ1, which occurred at 15-km focal distances (Figure 7 in the left) showed similar amplitude of the P first arrivals as the UD component in the surface seismometers. The S arrivals of EQ5 (M = 5.2) observed by the surface seismometers were 17 s later than the first P arrivals, but we were not able to identify the S arrivals in the DAS records in this event. EQ6, which was an aftershock of EQ5, showed similar waveforms. For EQ1 (Figure 7), the phase around the S arrival in DAS was probably an S phase. Although the temperature at the depth of 914 m was 264 °C, any distinct attenuation of the observed seismic waves was not observed in both earthquakes.

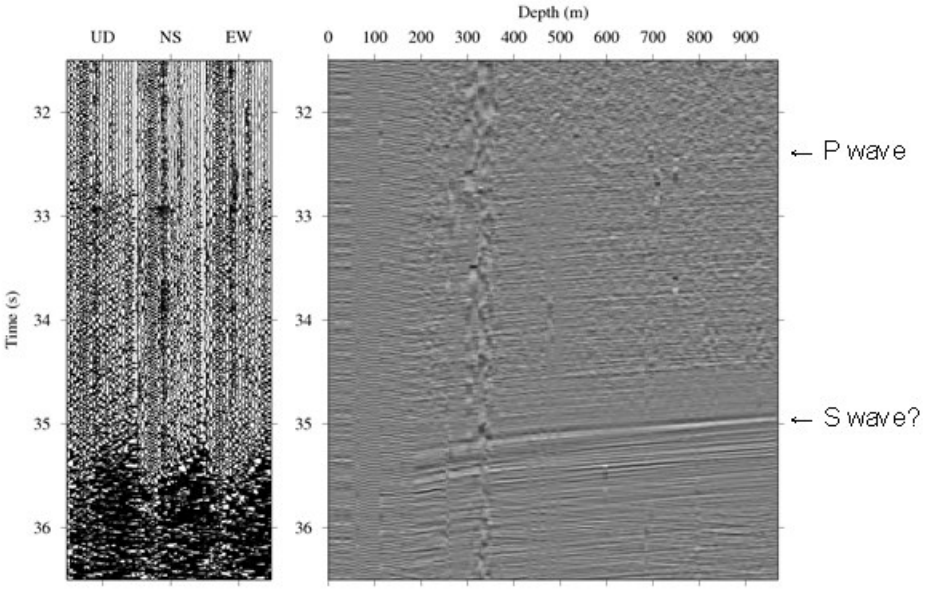

Figure 7: (Right) DAS records of EQ1 (M = 1.4, C in Figure 5). The horizontal axis indicates the depth in meters, and the vertical axis indicates the arrival time in seconds from 03:16, November 20, 2018. (Left) surface seismometer records. Each of the UD, NS, and EW is at a 1.9-km distance with 100-m spacing. The first P arrivals are identified from the depths of 977 to 200 m in the DAS records. The phase around the S arrival in DAS is probably an S phase.

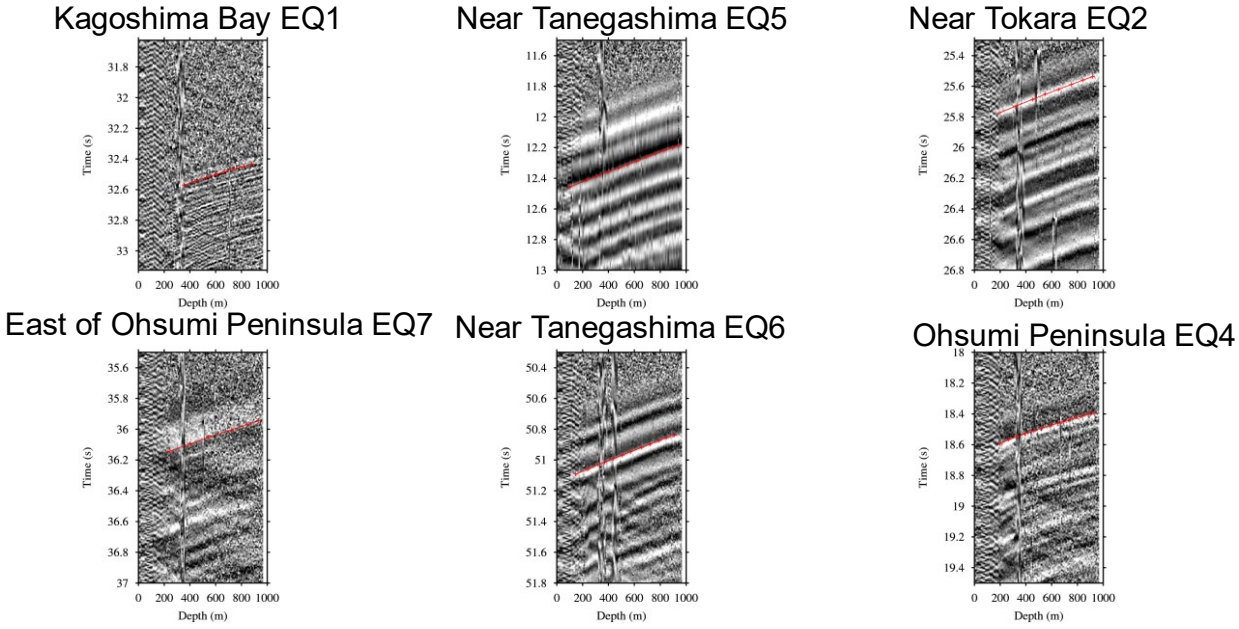

Figure 8: Observed DAS waveforms around the P arrivals in the six earthquakes. The red lines indicate the smooth fitting of the P arrival-time pickings to estimate the interval velocities.

We obtained the apparent interval Vp profile using the DAS records (Figures 8 and 9). A summary of the interval Vp profile is shown in Figure 10. Vp of the earthquakes from south of Medipolis between 200 and 977 m was approximately 3.0 km/s. On the other hand, the earthquakes from the north demonstrated velocities between 4.5 and 3.0 km/s in the depth range.

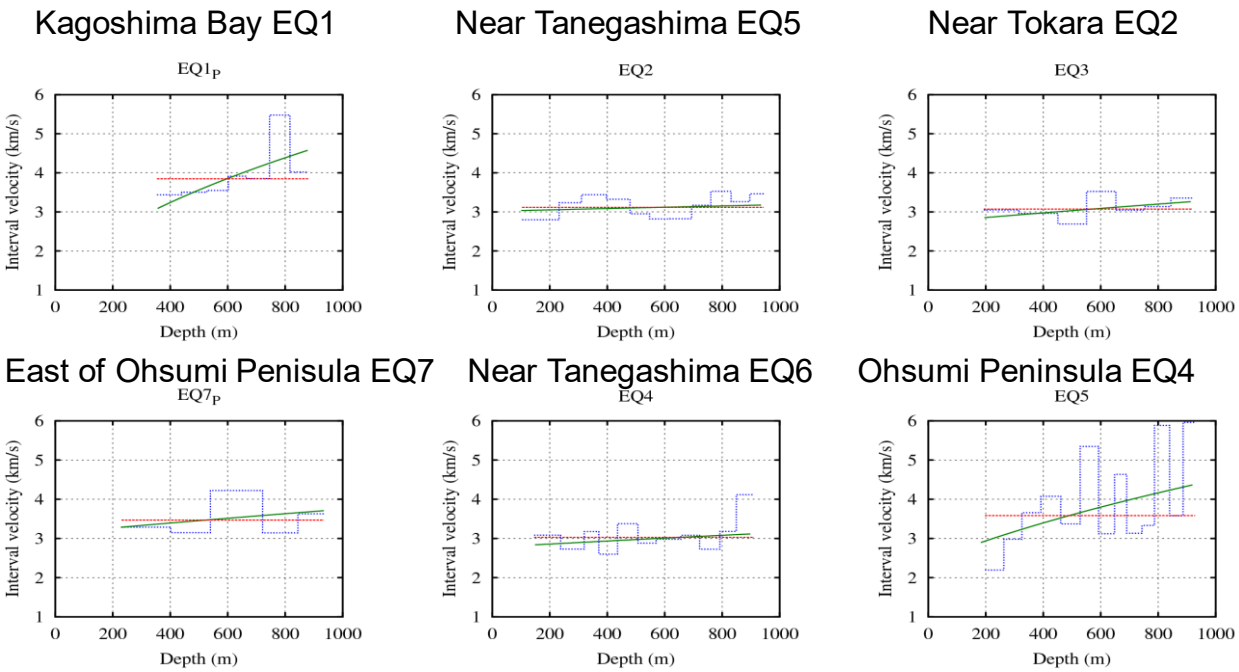

Figure 9: Results of the apparent interval Vp profile of the six earthquakes. The vertical and horizontal axes in each figure denote apparent interval Vp in km/s and the depth in meters, respectively. Green line: Vp obtained by the first arrivals fitted by smooth curves. Red line: mean Vp from the bottom to the shallowest depth. Blue line: Vp obtained by the picking of arrival times. EQ1 and EQ4 come from the north, and EQ2, EQ5, EQ6, and EQ7 come from the south.

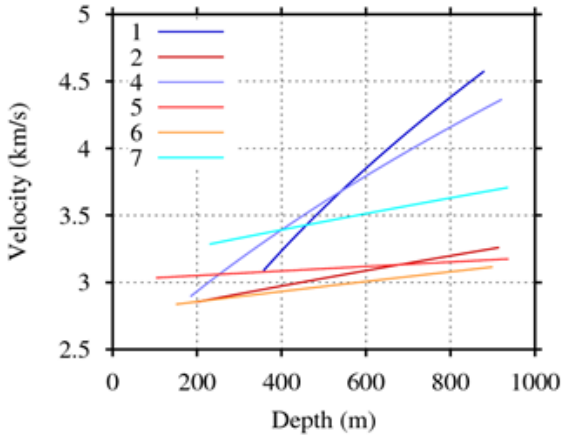

Figure 10: Summary of the apparent Vp depth profile of the six earthquakes. The line numbers correspond to the EQ numbers in Table 1. Two earthquakes (EQ1 and EQ4) exhibit larger velocity gradients with depth than those in the earthquakes from the south. Three earthquakes from the south (EQ2, EQ5, and EQ6) display an almost constant velocity of 3.0 km/s.

To explain the discrepancies in apparent interval Vp between the earthquakes from north and south, we evaluated the effect of the borehole deviation [shown in Figure 11 (left)]. The borehole deviation to the west started from a depth of 500 m, and it reached 70 m in the south. The azimuths of the incident seismic waves were from north to south corresponding to the earthquakes. We considered that Vp of the surrounding layer was 3.0 km/s for the depths from 0 to 1,000 m. When the seismic waves came from the south (azimuth 0°) with incident angle of 16°, apparent interval Vp was distributed between 3.15 km/s at the depth of 1,000 m and 3.0 km/s at the wellhead. When a similar case occurred in the north (azimuth 180°) and a 16° incident angle, apparent Vp was distributed between 3.5 and 3.1 km/s. When the incident angle was 30°, the Vp variation was between 4.3 and 3.5 km/s. Although we evaluated the ray paths in all earthquakes, the incident angles strongly depended on the hypocenters and shallow velocity structures near the borehole. Thus, the correct incident angles were difficult to estimate. Considering these problems, the current results shown in Figure 10 could be explained by the effect of the well deviation.

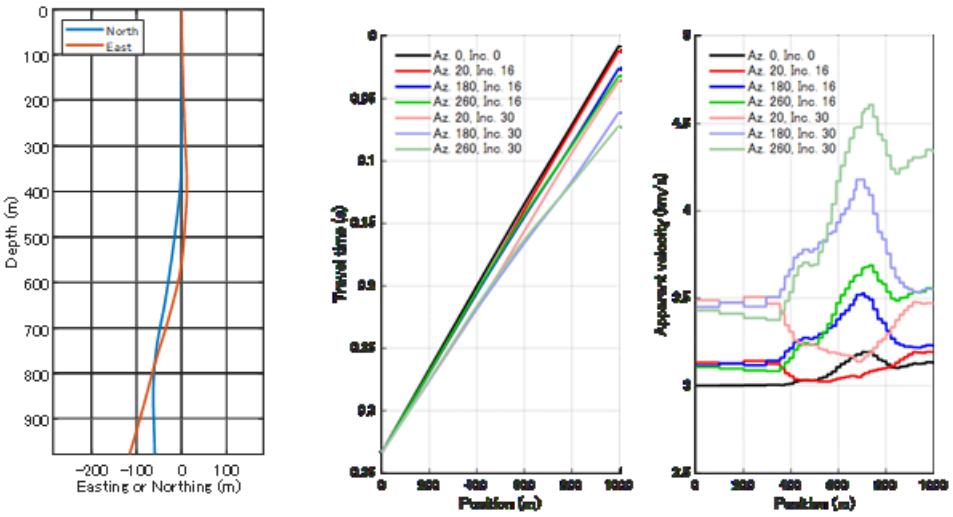

Figure 11: (Left) NS and EW deviations of the IK-4 borehole. The borehole deviates toward the west from the depth of 500 m to the bottom of the borehole (1,500-m deep). (Middle) We consider the case where Vp of the surrounding layer is 3.0 km/s. The apparent travel times from the bottom to the wellhead are shown at three incident angles and four different azimuths of the natural earthquakes. The azimuths of EQ2, EQ5, and EQ6 are approximately 0°, and those of EQ1 and EQ4 are approximately 180°. Two incident angles between 16° and 30° are considered. (Right) Apparent interval Vp profiles corresponding to the middle.

In some earthquake records, some surface seismometers showed a large arrival of the EW and NS components at 0.8 s after the first P arrivals of the vertical component (*e.g.*, EQ5 in Figure 12). Similar phenomenon was often seen by the OBS observations (Kasahara *et al.*, 1982). Such phase was interpreted to be a P-to-S conversion by the layer boundary between soft sediment and a hard-rock base. The large amplitudes of the horizontal components observed in this study were also considered as P-to-S conversion phases. The synthetic waveform estimation verified that this was caused by the P-to-S conversion at the Vp/Vs = 3 zone at an approximate deep of 4 km (Kasahara *et al.,* 2019b).

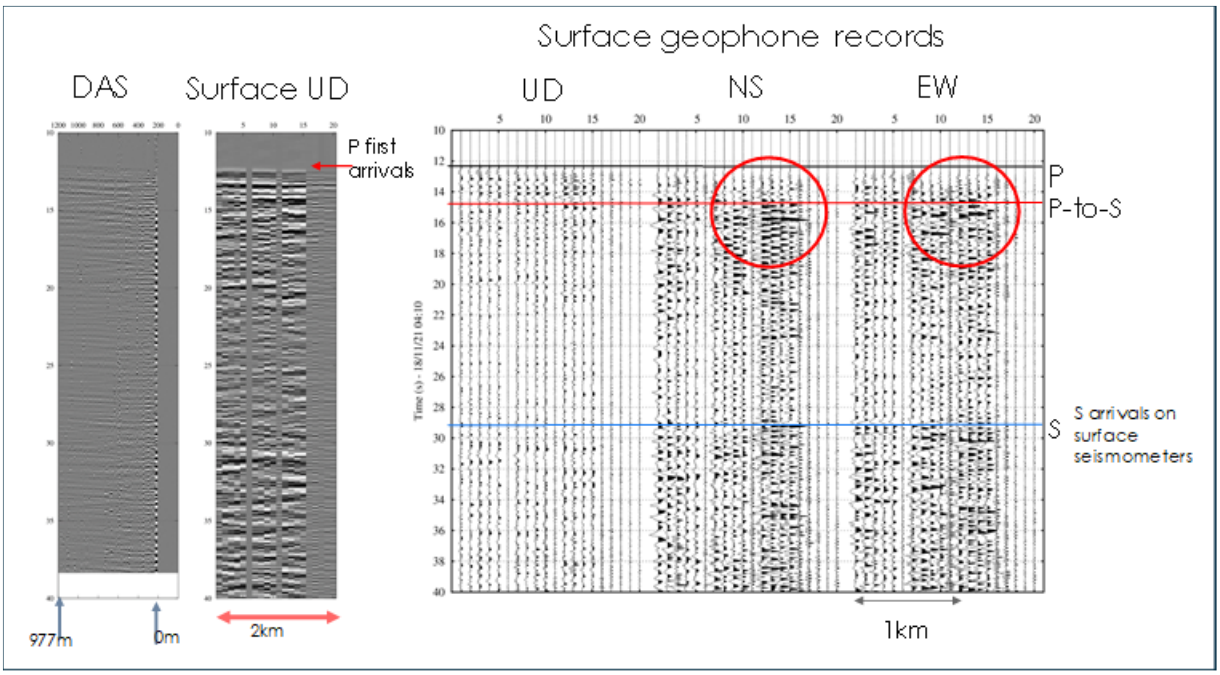

Figure 12: Possible P-to-S conversion arrivals seen in EQ5 observed by the surface seismometers. (Far left) DAS records. The vertical axis denotes the arrival time in seconds, and the horizontal axis denotes the distance. (Middle) UD component of the vertical component by the surface seismometer. (Far right) Surface seismometer records of UD, NS, and EW components. Each surface seismometer is located at 100-m spacing. Large amplitude arrivals are identified in the NS and EW components approximately 0.8 a after the first P arrivals observed in the UD component records.

A tremor-like noise was observed at a deep of approximately 350 m, and it disturbed the earthquake arrivals. Numerous kick-like events were observed (Figure 13). The earliest time suggested that the origin of events did not have the same depth for numerous events. One example of the kicks is shown in Figure 14. The duration time of this kick was very short. The earliest arrival was observed at 620 m and traveled upward and downward at 5 km/s. This velocity suggested that the seismic wave traveled through the casing pipes. The cause of the kicks could be acoustic emission or some extremely small bubbling.

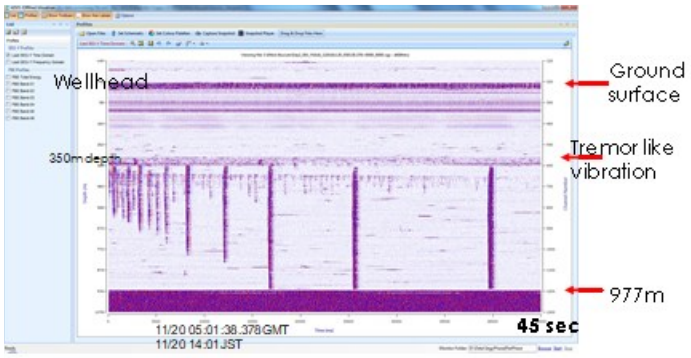

Figure 13: DAS 45-s-long records. The vertical axis indicates the depth, and the horizontal axis represents the time. The numerous vertical bars show the kick events.

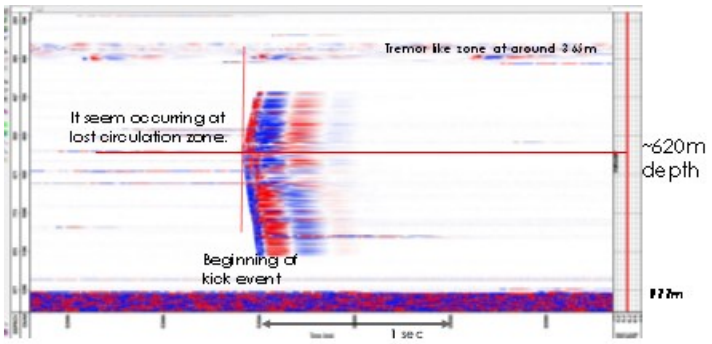

Figure 14: Enlargement of one of the kicks. The original depth of this kick is approximately 620 m and propagates upward and downward at 5 km/s.

4. DISCUSSION AND CONCLUSIONS

We carried out a feasibility study using the geothermal well in the Medipolis geothermal field. We measured the temperature and seismic waves in the IK-4 borehole down to a depth of 977 m using the DTS and DAS modes with the same optical fiber. The highest temperature was 264 °C at a depth of 914 m. In the DAS mode, we observed seven natural earthquakes that occurred near the Kyushu Peninsula. The sensitivity was comparable with that read by the surface seismometers. The result suggested that the optical-fiber deployment in the exiting borehole could provide reasonable coupling to the borehole casing. However, the S phase was not always detected because the incident angle of the earthquakes and the borehole were almost vertical. In addition, although we observed seven natural earthquakes, the incident angles of all earthquakes were almost vertical, and no reflected phases were observed from the deep intrusive body.

We estimated the apparent interval Vp profile using the records. The estimated interval Vp profile exhibited large discrepancies for cases involving north and south incident earthquakes. The south incident earthquakes exhibited lower Vp of approximately 3.0 km/s from the depth of 1,000 m to the wellhead. On the other hand, the north incident earthquakes exhibited Vp between 4.5 and 3.0 km/s at a depth of 1,000 m. The discrepancies among the earthquakes could be explained when we considered the deviation in the IK-4 well and the incidental angles and azimuth.

No significant attenuation in the P arrivals was observed in the DAS records around the highest temperature zone at the depth of 914 m. Between 800 and 977 m, the interval Vp profile in the borehole was 3.0 km/s, and it appeared to be less or not affected by the high-temperature zone. The reason for these results might be explained by the longer wavelength of the natural earthquakes because the dominant frequency of P was approximately a few hertz, the wavelength was on the order of kilometers, and the thickness of the high-temperature zone appeared to be less than a kilometer. If we use the higher frequency components provided by any sweep-type seismic source, we could observe the velocity dispersion depending on the thickness of the geothermal reservoirs.

The surface seismometer records suggested the presence of P-to S-converted waves, and the conversion could happen just below the Medipolis field. By using a large-size active seismic source, we could obtain the PP or PS reflection from the possible P-to-S conversion zone.

Tremor-like vibrations occurred at the depth of approximately 350 m. The cause of this tremor is under investigation. Numerous kick-like events were observed. The depths of the kick-like events were variable, and their cause needs further investigation.

ACKOWLEDGEMENTS

This study was supported by the New Energy and Industrial Technology Development Organization (NEDO). Medipolis Energy Co. charitably allowed the use of their IK-4 geothermal well for this study. Mr. Kimura provided us with the Schlumberger hDVS measurements. WELMA Co. provided us with the borehole fiber-optic system and measurement of temperatures in the borehole. The staff of West Japan Engineering Consultants, Inc., helped us during the field study.

REFERENCES

Bertani, R., Büsing H., Busk S., Dini A., Hjelstuen M., Luchini, M., Manzella A., Nybo R., Rabbe W., Serniotti. I. and the DESCRAMBLE Science and Technology Team: The first results of the DESCRAMBLE project, PROCEEDINGS, 43rd Workshop on Geothermal Reservoir Engineering Stanford University, Stanford, California, February 12-14, 2018 SGP-TR-213 (2018).

Daley, T. and B. Freifeld, B.: Advanced Monitoring Technology: DAS at Otway and Aquistore, IEA Greenhouse Gas Monitoring Network Edinburgh, Scotland (2016).

Dobson, P., Asanuma, H., Huenges, E., Pletto, F., Reinsch, T., and Sanjuan, B.: Supercritical geothermal system-A review of past studies and ongoing research activities, *Proceedings,* 42th Workshop on Geothermal Reservoir Engineering, Stanford University, Stanford, CA (2017).

Hartog, A.: "An Introduction to Distributed Optical Fibre Sensors", 442pp, CRC press (2017).

Kasahara, J., Nagumo, S., Koresawa, S., Nishi, Y., and Sugimoto, H.: A linear trend of hypocenter distribution in the outer slope region of the Japan Trench revealed by the OBS array-Preliminary report- Bull. Earthq. Res. Inst., Univ. Tokyo, **57**, 83-104 (1982).

Kasahara, J. and Hasada, Y.: "Time-lapse approach to monitoring oil, gas, and CO2 storage by seismic methods", Elsevier Pub., 201pp, (2016).

Kasahara, J., Takaichi, K., Suzuki, A., Yamaguchi, T., Mikada, H., Kitaoka, S., Fujise, Y.: Feasibility study of super critical water reservoirs for the next generation of clean and renewable energy sources, JPGU 2018 annual meeting abstract (2018a).

Kasahara., J, Hasada, Y. and Yamaguchi. T.: Full-wave seismic imaging of super critical geothermal reservoir, Proc. Of 138th SEGJ conference, Tokyo, Japan (2018b).

Kasahara, J., Hasada, Y. and Yamaguchi, T.: Seismic time-lapse approach to image the oil, gas and geothermal reservoirs and CO_2 storage zones, Abstract, "Recent Advances and applications in borehole geophysics", SEG Summer Research Workshop, August 27-30, 2018, Galveston, USA. (2018c).

Kasahara., J, Hasada, Y., Kawashima, H., Sugimoto, Y., Yamauchi, Y., Yamaguchi, T. and Kubota, K.: Comparison of DAS (distributed acoustic sensor) and seismometer measurements to evaluate physical quantities in the field, ACQP2, Expanded abstract of SEG 2018 annual meeting, Anaheim, U.S.A. (2018d).

Kasahara, J., Hasada, Y., and Yamaguchi, T.: Seismic imaging of supercritical geothermal reservoir using full-waveform inversion method, *Proceedings,* 43th Workshop on Geothermal Reservoir Engineering, Stanford University, Stanford, CA (2019a).

Kasahara, J., Hasada, Y., and Kuzume, H., 2A possible geothermal source at around 4 km depth estimated by the seismic observation in Ibusuki geothermal area, JPGU 2019 annual meeting abstract SVC39-03 (2019b) .

Mellors, R., Sherman, C., Ryerson, R., Morris, J., Messerly, M., Yu, C., Allen, G. and Ichinose, G.: Modeling Potential EGS Signals from a Distributed Fiber Optic Sensor Deployed in a Borehole, *Proceedings,* 42th Workshop on Geothermal Reservoir Engineering, Stanford University, Stanford, CA (2018).

Muraoka, H., Uchida, T., Sadada, M., Yagi, M., Akaku, K., Sasaki, M., Yasukawa, K., Miyazaki, S., Doi, N., Saito, S., Sato, K. and Tanaka, S.: Deep geothermal resources survey program: Igneous metamorphic and hydrothermal processes in a well encounterizing 500°C at 3729m depth, Kakkonda, Japan., Geothermics, 27(5/6), 507-534 (1998).

NEDO: Report of Geothermal Development Promotion, East of Ikeda Lake No. C-2-10, First, Second and Third phases, 2008, 2009, 2010.

Patterson, J., Cardiff, M., Colemman, T., Wang, H., Feigl, K. L., Akerly, J. and Spelman, P.: Geothermal Reservoir Characterization Using Distributed Temperature Sensing at Brady Geothermal Field, Nevada, *Proceedings,* 42th Workshop on Geothermal Reservoir Engineering, Stanford University, Stanford, CA (2018).

Rabbel, W.: Seismic Exploration of a Deep, Possibly Super-critical, Hydrothermal Reservoir in the Larderello Area, in WS09 Exploration and Monitoring of Geothermal Reservoirs Workshops, EAGE 2019 Annual Meeting, London (2019).

Reinsch, T., Dobson, P., Asanuma, H., Huenges, E., Pletto F. and Sanjuan, B.: Utilizing supercritical geothermal systems: a review of past ventures and ongoing activities, Geothermal Energy, 10175:16 (2017) https://doi.org/10.1186/s40517-017-0075-y.

Trainor-Gutton, W., Gutton, A., Jrelf, S., Powers, H., Simmons, C., Sullivan, C. B. and POROTOMOTO Team: Imaging from Vertical DAS Fiber at Brady's Natural Laboratory, *Proceedings,* 42th Workshop on Geothermal Reservoir Engineering, Stanford University, Stanford, CA (2018).